Finite Element Modeling of Axially Loaded CFRP-Confined Rectangular Reinforced Concrete Columns

Hamed Akbarpour [a*], Masoumeh Akbarpour [b]

[a] Department of Civil and Environmental Engineering, The Pennsylvania State University, University Park, USA

[b] Department of Civil Engineering, K.N. Toosi University of Technology, Tehran, Iran

Abstract

This paper investigates numerically the behaviour of rectangular RC columns strengthened with carbon fiber reinforced polymer (CFRP) composites under uniaxial loading. For this a reason, a parametric study is conducted and the effects of CFRP layers number, compressive strength of unconfined concrete, and fiber orientation on the behaviour of such columns have been studied. The number of CFRP layers has been changed from one to five layers while the fibers are oriented transversely. Compressive strength of unconfined concrete has been increased from 26 MPa to 45 MPa. In addition, three different fiber orientations are considered. The results show that an increase in the number of CFRP layers would enhance the ultimate strength of specimens. Although increasing the number of layers would not increase the ultimate strength of specimens exponentially, but the rate of strength gain would also decrease. Moreover, it is shown that lateral strains increase as the layer number increases. The effect of unconfined concrete strength on the ultimate strength is less for low strength concrete than high strength concrete. Evaluating the effect of fiber orientation shows that the maximum ultimate strength is obtained from transverse orientation and as the angle of orientation increases, the ultimate strength decreases.

Keywords: Axial Load; Rectangular Concrete Columns; Carbon Fiber Reinforced Polymer; Strength; Ductility.

1. Introduction

In recent years, fiber-reinforced polymers (FRPs) are used widely for strengthening reinforced concrete (RC) columns to achieve more strength and ductility. Under the lateral confining pressure provided by FRPs, such columns are subjected to a tri-axial stress state and consequently the total strength and ductility increase [1, 2].

Most of studies reported in the literature are devoted to the investigation on the behavior of circular RC columns under axial load, but fewer attempts are made on square/rectangular RC columns. In non-circular RC columns, the compressive strength of confined concrete is a function of the cross-sectional aspect ratio, the height, the corner radius, the unconfined concrete strength, the longitudinal and transverse reinforcement ratio, and the mechanical properties of FRPs.

Wu et al. [3] presented the results of an experimental study on the behavior of axially loaded rectangular columns. 45 specimens were tested under uniaxial compression where the effects of the cross-sectional aspect ratio and the number of CFRP layers were studied. The test results indicated that the strength gain in the confined columns decreased as the aspect ratio increased, but the aspect ratio of 2 was a limit point where its effect became insignificant. It is also showed that an increase in the FRP layers lead to increase the strength and ductility of specimens.

El-Hacha et al. [4] investigated the slenderness effects of confined concrete with CFRP. 18 specimens with varying slenderness ratio tested under axial loading up to failure. The results showed that increasing the height of columns reduced the ultimate axial strength where this reduction is more significant for the wrapped columns.

Al-Salloum [5] evaluated the effect of the corner radius on the strength of square RC columns confined with FRP sheets. 20 specimens were built and tested under axial loading up to failure. Corners were rounded to 1/6, 1/4, and 1/3 of the side dimension and the minimum radius was considered as 5 mm. The results showed that the efficiency of FRP sheets was related to the corner radius and improved the strength and ductility.

Chaallal et al. [6] carried out a comprehensive experimental investigation indicating the effects of the concrete strength, the aspect ratio and the number of CFRP layers on the behavior of axially loaded short rectangular columns. A total of 90 specimens were tested under axial compression and the results showed that the maximum gain in strength and ductility can be achieved for lower strength concrete than for normal-to-high strength concrete. Generally, as unconfined concrete strength increased, both axial and transverse strains decreased, that is, the gain in ductility decreased.

This paper presents the results of a numerical study on the behavior of axially loaded CFRP-confined rectangular RC columns using finite element analysis software, ANSYS. The effects of parameters like the unconfined concrete strength, the number of CFRP layers, and the fiber orientation on the behavior of RC columns are studied.

2. Modeling and Analysis

This paper presents the results of a numerical study on the behavior of CFRP-confined rectangular RC columns under concentric compression using ANSYS. At first, the modeling procedure is verified with an experimental study, and then a parametric study is carried out. This procedure is expressed in the following.

2.1. Description of Model

A specimen is selected from an experimental study reported by Ilki et al., (NS-R-2-175-3-40) [7]. NS, R, 2, 175, 3, and 40 are representative of normal strength concrete, rectangular cross-section, cross-sectional aspect ratio, distance between transverse reinforcements in the test zone, CFRP layers number, and the corner radius, respectively. Geometry, dimensions, and reinforcing arrangement of the specimen are shown in Figure 1. It is noted that all dimensions are given in millimeter.
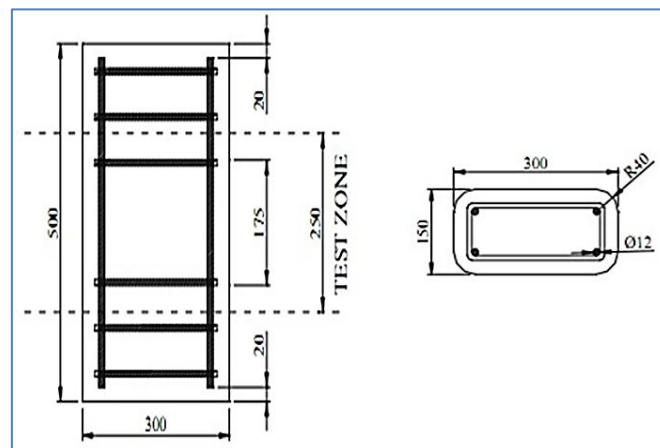

Figure 1. Geometry and reinforcing arrangement of NS-R-2-175-3-40 [7]

Unidirectional carbon fiber-reinforced polymer composite is used to strengthen the specimen. The CFRP composite has a linear elastic behavior up to rupture and then is modeled as a linear orthotropic material. The material properties of CFRP composite are summarized in Table 1. Longitudinal and transverse reinforcements' diameters are 12 and 8 mm, respectively and are modeled with bilinear isotropic hardening plasticity. The mechanical properties of the reinforcements are given in Table 2.

Table 1. Material properties of CFRP composites

Material	Elastic Modulus (GPa)	Tensile Strength (MPa)	Ultimate Strain (%)	Thickness per layer (mm)	Unit Weight (Kg/m^3)
Carbon/Epoxy	230	3430	1.5	0.165	1820

Table 2. Material properties of steel reinforcements

Nominal Bar Diameter (mm)	Yield Strength (MPa)	Yield Strain
8	476	0.0024
12	339	0.0017

Unconfined concrete strength (f'_{co}), Poisson's ratio (v), and ultimate strain of unconfined concrete (ϵ_{co}) are 26.4 MPa, 0.2, and 0.003 mm/mm, respectively. The confining pressure of CFRP-confined rectangular RC columns is modeled with the Drucker-Prager yield criterion. This criterion is a smooth approximation of the Mohr-Coulomb yield surface, which is a function of cohesion, angle of internal friction, and dilatancy angle. It is noted that there is not a general rule to determine these parameters, thus the empirical formulas are used as follows [8]:

$$c = (f'_{co} - 5\sqrt{3})\frac{3 - \sin\varphi}{6\cos\varphi} \tag{1}$$

$$\varphi = \sin^{-1}(\frac{3}{1 + \frac{0.4 f'_{co}}{\sqrt{3}}}) \tag{2}$$

Where c is cohesion in MPa and φ is friction angle in degree.

The dilatancy angle is an important parameter affecting yield behavior of the specimen. It changes from zero to the angle of internal friction. When it is equal to zero, no volume expansion is occurred and when it is equal to the angle of internal friction, volume expansion and plastic strains would happen. In this research, a sensitive analysis is done on the dilatancy angle to gain more adaption between the numerical and experimental results.
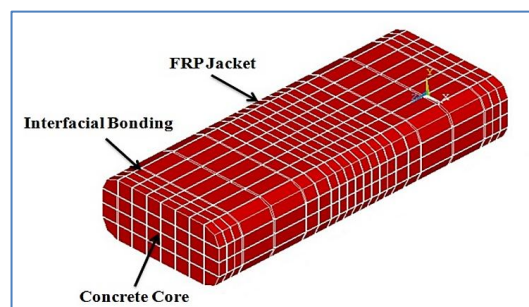
2.2. Reagents and Materials

Crude oil, sand, and bentonite were supplied from Tehran Oil Refinery, Silica Sand MFG Company, and Mokarrar Composite Company, respectively. The sandy soil was synthesized by mixing equal amounts of two sand types (foundry mold sand 141 and industrial sand D11). Table 1. shows a brief description of the resulting mixture characteristics. Moreover, Particle size analysis was performed in case of the soil according to ASTM D422-07. Figure 1. illustrates the grain size distribution of the soil sample. According to the grain size distribution, values of d_{10}, d_{60}, and d_{30} were obtained; consequently, C_u and C_c were calculated.

Oil is a liquid with a complex mixture of organic molecules with varied chemical and physical properties. In the case of oil-contaminated soils, the influence of oil on the behavior of soil mainly depends on the type of oil and soil particles. Therefore, the type of oil is one of the important factors that affect the angle of internal friction and interface friction angle of sand. Crude oil specifications are tabulated in Table 2.

2.3. Finite Element Model and Meshes

A 3-D model of confined RC columns is built using ANSYS. The model is meshed with different elements for each material, and specific properties are assigned. A total of 8976 nodes and 1848 elements have been used to mesh the specimens. The meshed model is shown in Figure 2. For concrete, an 8-node solid brick element, SOLID65, is used which has three translation degrees of freedom per node. This element has capabilities of cracking in tension and crushing in compression and is useful for modeling the nonlinear behavior of materials. Solid65 also able to model three rebar materials within the concrete but this capability is not considered. All steel reinforcements are modeled with a 2-node link element, LINK8. This element has three translation degrees of freedom per node and a perfect bond between the concrete and steel reinforcement nodes is assumed. The geometry and element coordinate system of these elements are shown in Figures 3 and 4 [9].

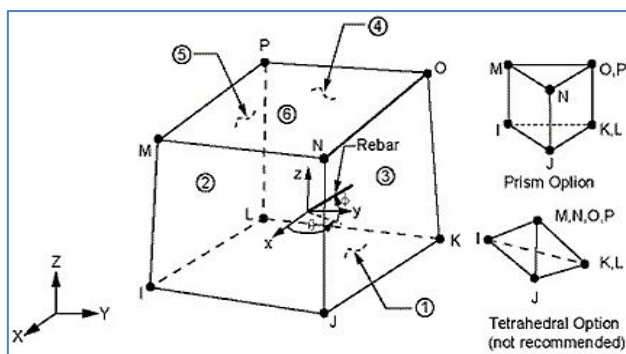**Figure 2. Geometry and element coordinate system of SOLID65 [9]**

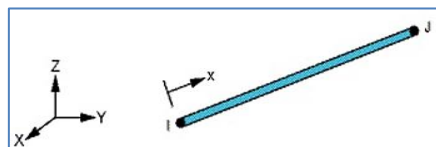**Figure 3. Geometry and element coordinate system of SOLID65 [9]**

Figure 4. Geometry and element coordinate system of LINK8 [9]

A 4-node shell element, SHELL181, is used to define the CFRP composites. This element has six degrees of freedom at each node, but its membrane behavior is considered. Thus, the degrees of freedom decrease to three translation degrees in X, Y, and Z directions. The geometry and element coordinate system of this element is shown in Figure 5 [9].
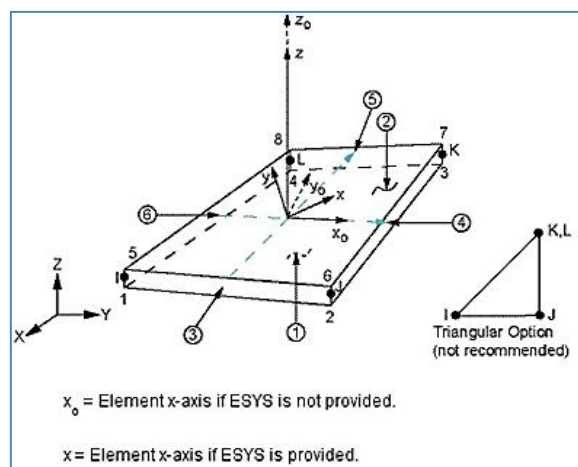

Figure 5. Geometry and element coordinate system of SHELL181 [9]

The interface between CFRP sheet and concrete is modeled by a 2-node contact element, CONTA178. This node-to-node 3-D contact element has three degrees of freedom at each node and an initial gap capability. The geometry and element coordinate system of this elements are shown in Figure 6 [9].
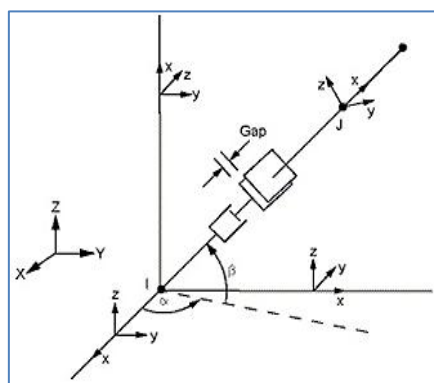

Figure 6. Geometry and element coordinate system of CONTA178 [9]

2.4. Boundary Conditions

Due to symmetry in geometry and loading of the columns, only 1/8 of specimens are modeled and symmetry boundary conditions are exerted on the x-y, x-z, and y-z planes. In this regard, the translation degree of freedom for each node of symmetrical planes is clamped on the perpendicular direction to the planes. The degrees of freedom of all displacements of the nodes in the top surface are coupled. The displacements are applied on all nodes on the top surface (in z direction) in several load steps and sub-steps.

2.5. Model Interactions

One of the key parameters in modeling the behavior of CFRP-confined rectangular RC columns is how to correctly model the interface surface between concrete and CFRP composites. In this regard, the coefficient of friction on the interfacial bonding surface is changed from zero to one. The amount of zero represents a fully interfacial bonding whereas the one shows that there is not a sufficient bonding. The variation in axial stress vs. axial strain based on a change in the coefficient of friction is shown in Figure 7.
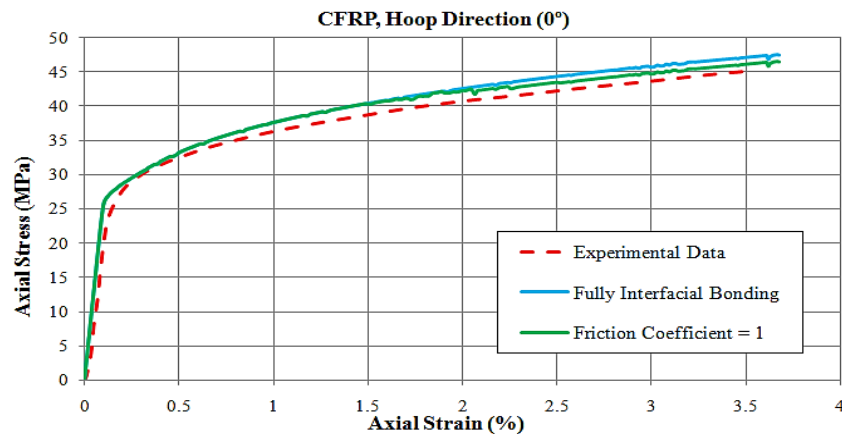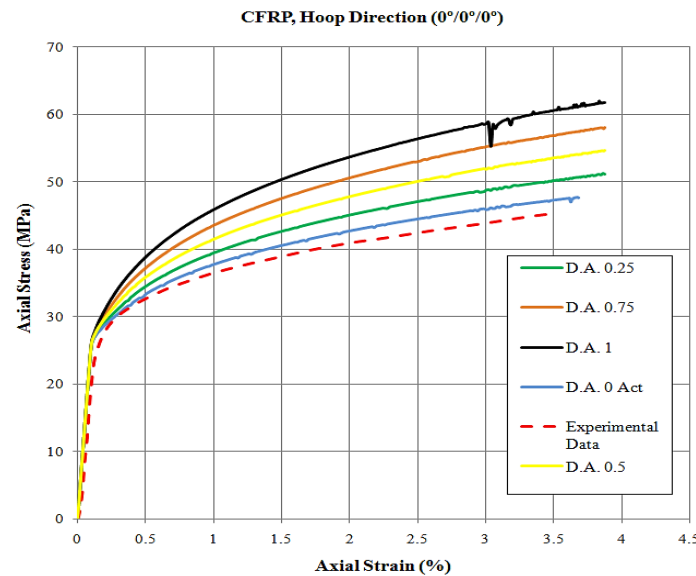

Figure 7. Effect of friction coefficient on axial stress-axial strain diagram

The results indicate that changing coefficient of friction does not have a significant effect, therefore, concrete and composite will spill simultaneously in ultimate state. For this reason, the contact elements have been omitted and the nodes of concrete and composites merged together.

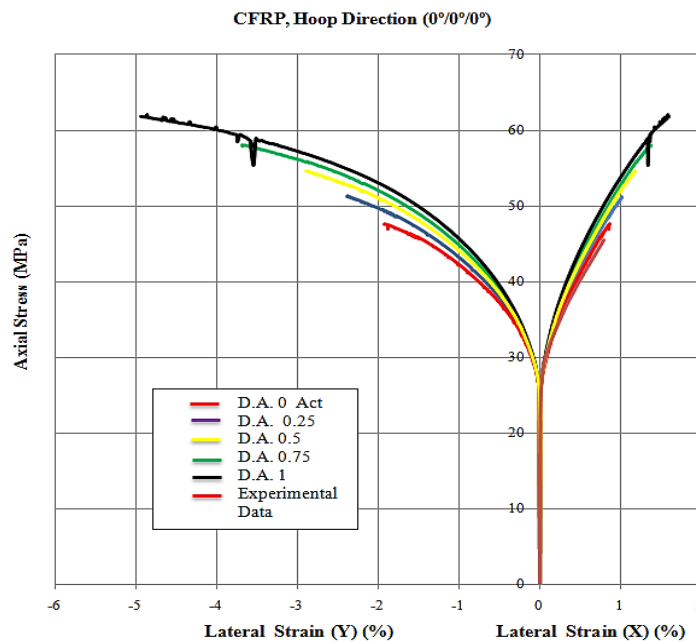### 2.6. Sensitive Analysis on the Dilatancy Angle

The applied load is divided to some load steps and Newton-Raphson equilibrium iterations provide convergence at the end of each load step. In this nonlinear static analysis, two tolerance limits of displacement and force are assumed 0.05 and 0.001, respectively.

Before continuing the analysis, it is necessary to conduct a sensitive analysis on the dilatancy angle, because it is a considerable parameter in Drucker-Prager yield criterion for modeling CFRP-confined RC columns. This parameter shows the amount of plastic volume strain, which is constant in the plastic region. In this project, the dilatancy angle is changed from zero to the angle of internal friction. The ratio of dilatancy angle to angle of internal friction is considered as 0, 0.25, 0.5, 0.75 and 1.0. The effect of dilatancy angle on axial stresses, axial strains, and lateral strains in both x and y directions is shown in Figures 8 and 9.

Figure 8. Effect of dilatancy angle on axial stress-axial strain diagram

In Figure 8, the vertical axis is the axial stress in MPa and the horizontal axis is the axial strain. The results show that as the dilatancy angle increases, slope of secondary region also increases representing the effect of CFRP layer on the behavior of confined concrete. Such increase in the secondary region indicates an improvement in the axial stress of confined concrete. It is also noted that every change in dilatancy angle leads to a shift in the yield surface of Drucker-Prager model and the plastic capacity of columns, so the change does not affect the slope of the linear elastic region. A comparison shows that the dilatancy angle of zero results in good prediction of the mentioned experimental study.

Figure 9. Effect of dilatancy angle on axial stress-lateral strains diagram

Increasing the dilatancy angle also increases the slope of axial stress - lateral strains diagram in both X and Y directions. The increase in the direction of larger side (X) is lower than the little side (Y). It also increases significantly the lateral strain in the direction of little side due to confining deficiency produced by CFRP composites. As the cross-sectional aspect ratio increases, the deficiency of CFRP enhances enabling the concrete to reach a higher level of plastic capacity where the dilatancy angle increases. As shown in Figure 9, the dilatancy angle of zero has the best consistence with the experimental study.

3. Results and Discussion

This paper presents the results of a parametric study on the behavior of rectangular RC columns strengthened with the CFRP composites under axial loading. The effects of parameters like the thickness of composites, the unconfined concrete strength and the orientation of fibers on the behavior of such columns are discussed as follows:

3.1. CFRP Thickness

The effect of CFRP layers on the behavior of confined columns is discussed herein. For this reason, the strength of unconfined concrete is assumed to 26 MPa and the number of layers is changed from 1 to 5 layers, while all other material properties are constant. It is noted that ANSYS has a capability to define different number of layers with different fiber orientation for a shell element. The results are shown in Figures 7 - 13.

In Figure 10, the first region is not affected by a change in the number of layers, which represents an elastic behavior of concrete. Then, a transition region starts by producing micro-cracks, where an increase in the CFRP layers enhances the stresses. It is noted that this improvement in the stress state is not significant due to the limited confining pressure exerted by the composites to the concrete core. In the third region, the CFRP sheet confines the concrete effectively and the stiffness has been stabled with a constant rate. So the slope of this section is governed basically by the number of layers, because the concrete core does not remain homogenous after cracking and the volume expansion transfers directly to the CFRP composites. As shown in Figure 9, as the number of layer increases, the slope of the third region increases as well. The results show a change in the layer number from 1 to 5 increases the ultimate stress to 40.15 MPa, 44.49 MPa, 47.04 MPa, 49.18 MPa and 50. 45 MPa, respectively. In fact, the ultimate strength of confined to unconfined concrete ratio is 1.54, 1.71, 1.81, 1.89 and 1.94, respectively. As mentioned above, the gain of ultimate strength increases due to the presence of CFRP composites, but as the layer number enhances the amount of strength obtained decreases. In other words, the strength gained is constant after a determined number of layers which is related to how the cross-section of columns is confined effectively. In the middle part of each side, confinement is insignificant and increasing the number of layers would have a little impact on this part. So adding more and more layers would not have a significant effect on the amount of gain in total strength of the specimens. The reason is rupturing of CFRP layers at the corners of the section and high stress concentration at these parts. The gain obtained from increasing the CFRP layers is shown in Figure 11.
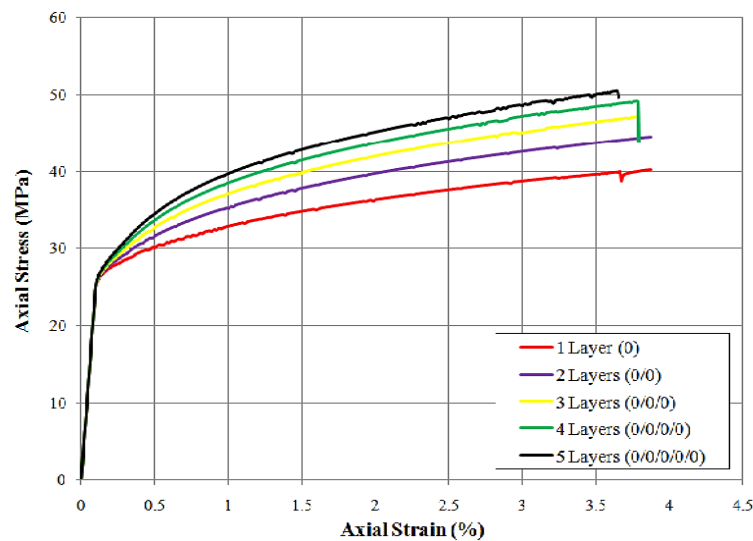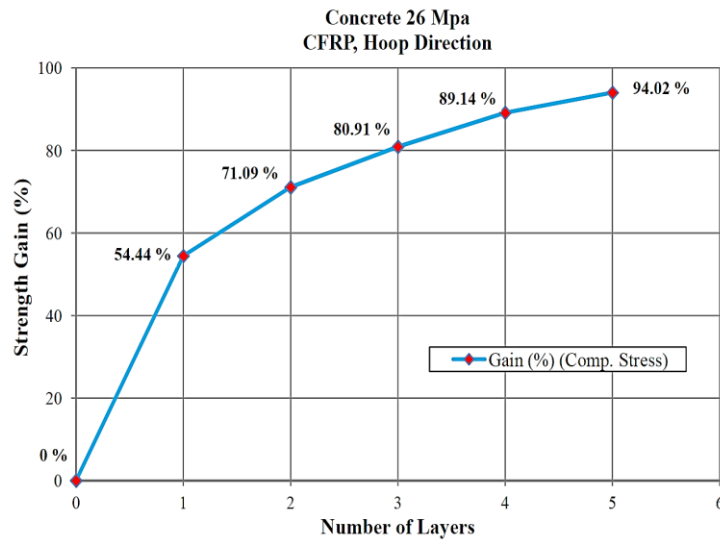

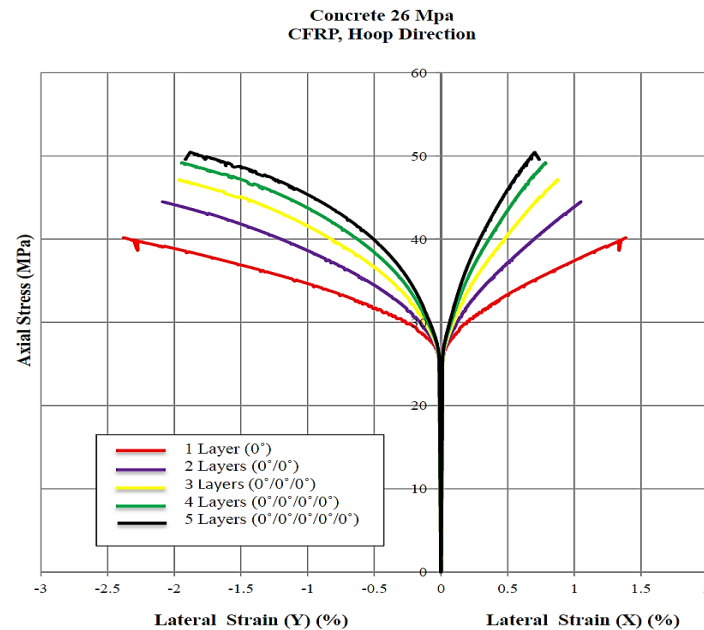**Figure 10. Effect of CFRP layers on axial stress-axial strain diagram**

In Figure 10, it is shown that an increase in the number of CFRP layers would not affect compressive axial strain significantly and all specimens have failed at an average axial strain of 3.789 percent. It is also clear that strengthening specimens with CFRP layers has increased their ductility, because the strain corresponding to maximum compressive strength in an unconfined concrete was 0.2 percent.

Concrete 26 Mpa
CFRP, Hoop Direction

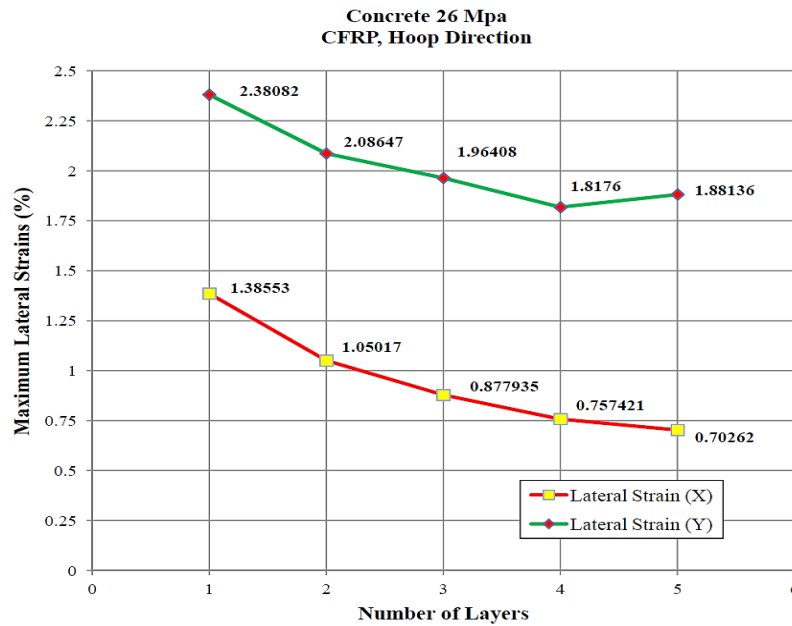**Figure 11. Strength gain rate based on the number of CFRP layers**

In general, strength and ductility of unconfined reinforced concrete columns are low and CFRP confinement would improve their properties. When cracking has been started, concrete starts expansion resulting in the activation of CFRP layers and then applying confining pressure to the concrete. The pressure is a function of lateral strain of concrete, which is related to axial strain of concrete core. As axial and lateral strains increase, axial compressive strength of specimens increases. As shown in Figure 12, increasing the number of layers increases lateral strains of confined concrete with low compressive strength. It is clear that the effect of confinement is more in the direction of smaller side than the longer side. However, it should be noted that increasing CFRP layers decreases lateral strains.

Concrete 26 Mpa
CFRP, Hoop Direction

Figure 12. Axial stress versus lateral strains in the direction of two sides of the cross section

Maximum lateral strains in direction of cross-section's sides are shown in Figure 13. As shown, the rate of increase in lateral strain in the direction of longer side of the cross section tends to a constant value by increasing the number of layers. This shows that increasing the number of layers will not lead to an excess in the dilatancy ratio with respect to a specific value.
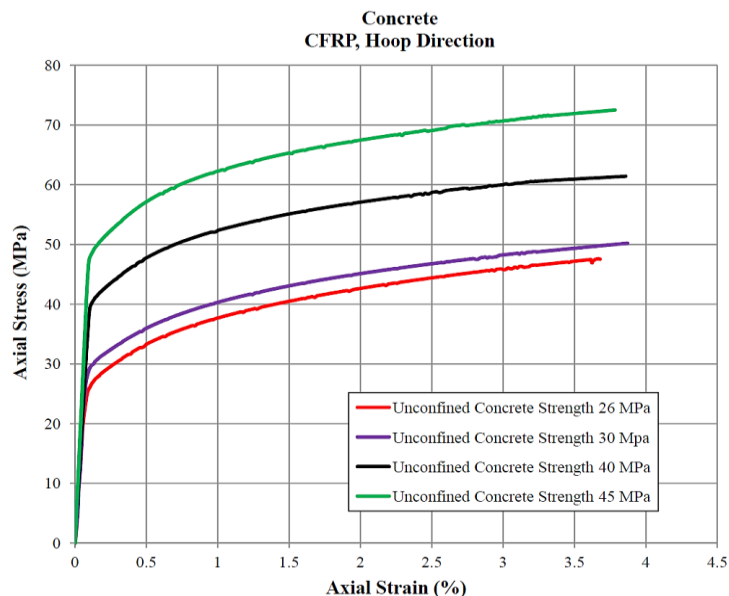
Figure 13. Variation of lateral strains in the direction of two sides of the cross section with respect to increasing the number of CFRP layers

3.2. Compressive Strength of Unconfined Concrete

To evaluate the effect of compressive strength of unconfined concrete on the behavior of CFRP-confined rectangular reinforced concrete columns, it has been changed from 26 MPa to 45 MPa. The results show as compressive strength of unconfined concrete increases, stress corresponding to failure point in a bilinear axial stress-strain diagram increases. In addition, stress in transition zone is also increased. It is also noted that the ultimate strength of confined specimens with a low compressive strength of unconfined concrete would not change significantly. However, for high strength concrete, the ultimate strength would increase slightly so that it would be 47.54 MPa and 50.17 MPa, respectively, for unconfined concrete compressive strengths of 26 MPa and 30 MPa. But the corresponding values for compressive strengths of 40 MPa and 45 MPa would be 61.41 MPa and 72.51 MPa, respectively (Figure 14).

Figure 14. Effect of compressive strength of unconfined concrete on axial stress-axial strain diagram

Figure 14. shows the effect of compressive strength of unconfined concrete on the ultimate strength of CFRP-confined specimens. As shown, as compressive strength of unconfined concrete increases, the efficiency of CFRP layers decreases. For example, the gains in compressive strength are 82.83%, 67.25%, 53.52%, and 61.13% for unconfined concretes with compressive strengths of 26 MPa, 30 MPa, 40 MPa, and 45 MPa, respectively. It is clear

that the effect of confinement on the concrete with low compressive strength is more than that of high strength concrete.

Figure 15. shows axial stress-lateral strains diagrams for a confined rectangular reinforced concrete column with different compressive strength of unconfined concrete. As shown in Figure 15, as compressive strength of unconfined concrete increases the corresponding lateral strains decrease. The reason is an increase in the column's rigidity which is induced by higher compressive strength of concrete. A decrease in lateral strains of concrete core results in lower tensile strains in CFRP layers. Hence, lower confining pressure would be exerted to the concrete core and then the efficiency of CFRP layers decreases. An increase in compressive strength of unconfined concrete decreases the gains in strength obtained and the efficiency of CFRP layers. Moreover, increasing compressive strength of unconfined concrete does not influence ultimate axial strain of columns significantly.
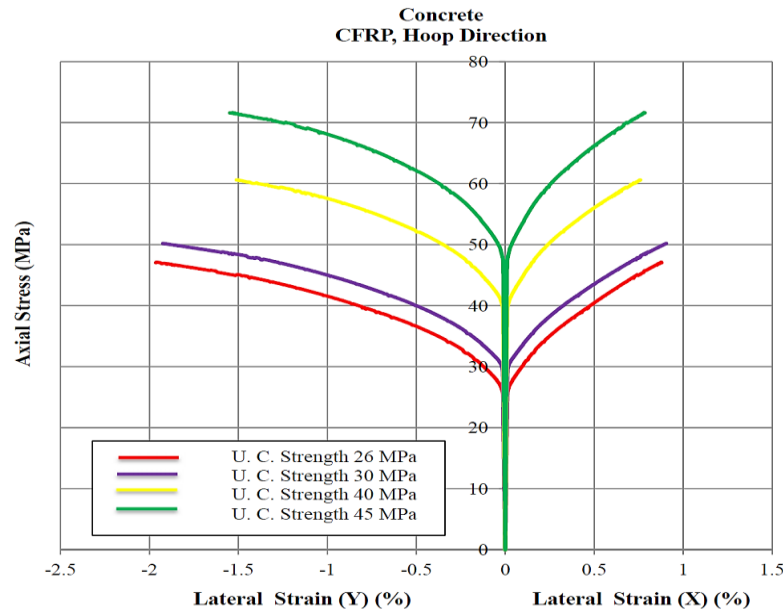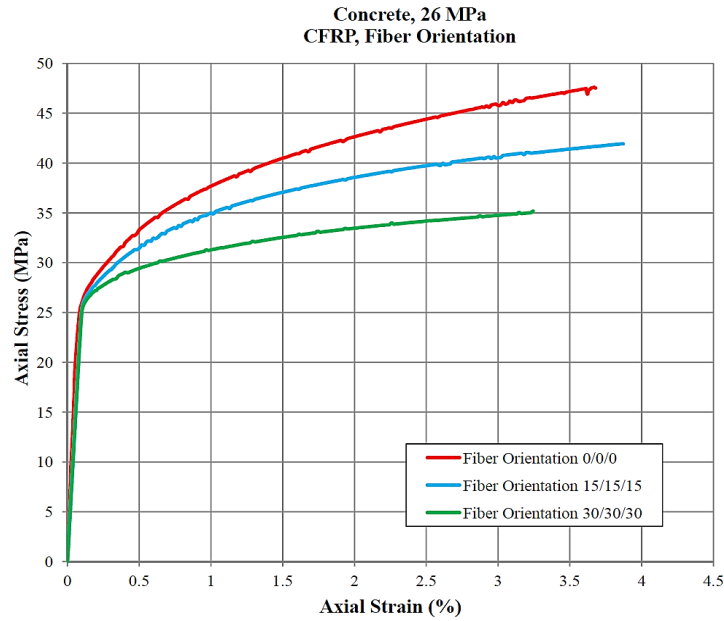

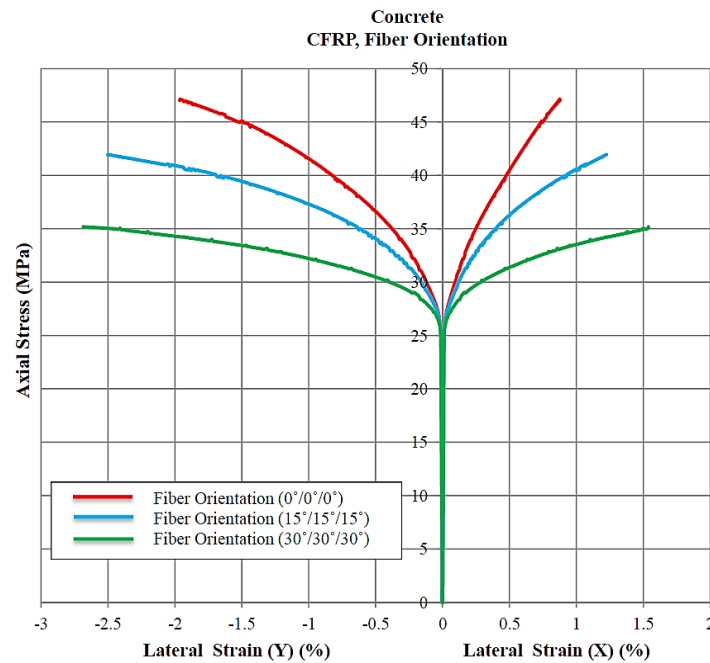**Figure 15. Effect of compressive strength of unconfined concrete on axial stress-axial strain diagram**

3.3. Fiber Orientation

In this project, three fiber orientations of $(0)_3$, $(15)_3$ and $(30)_3$ are considered. The first orientation represents a transverse orientation of fibers and all other orientations are calculated from this direction. Figure 16 shows axial stress-strain diagrams for theses fiber orientations. As shown, maximum gain in strength is obtained from transverse orientation. As the angle of fibers increases, ultimate strength of confined concrete decreases. For example, ultimate strength for the transvers orientation is 47.54 MPa, but it decreases to 35.18 MPa for the third orientation. However, the amount of axial strain or ductility for the second orientation is more than others.

It is noted that as the confinement of concrete core decreases, lateral strains of columns increase before reaching the failure mode. At the failure point, the CFRP layer is ruptured at the corners of the cross section. This behavior is shown in Figure 17. As shown, the slopes in the curves of smaller side are more than those of longer side. Lateral strains in the direction of longer side are more than those of the other side because confining pressure decreases.

Figure 16. Effect of fiber orientation on axial stress-axial strain diagram

Figure 17. Effect of fiber orientation on axial stress-lateral strains diagram

4. Conclusion

This paper presents the results of a numerical study on the behaviour of CFRP-confined rectangular reinforced concrete columns under axial loading. The results show that an increase in the number of CFRP layers would enhance the strength of columns. But, it is noteworthy that as the CFRP layers increase, the strength gains rate decreases. This means that there is an optimum point for the number of layers to work efficiently. In addition, increasing the unconfined concrete strength from 26 MPa to 45 MPA results in an increase in the ultimate strength of columns. Also, it decreases the lateral strains and ductility. Moreover, the maximum ultimate strength is achieved when fibers are oriented in a transverse direction. As the angle of orientations increases, the ultimate strength decreases while ductility increases.

5. References

[1] Rahai, A., and Akbarpour, H. "Experimental investigation on rectangular RC columns strengthened with CFRP composites under axial load and biaxial bending", Composite Structures 108 (2014): 538-546.

[2] Rahai, A., and Akbarpour, H. "Biaxially loaded CFRP-confined rectangular RC columns", Proceedings of the Thirteenth East

Asia-Pacific Conference on Structural Engineering and Construction (EASEC-13), 2013.

[3] Wu, YF, and Wei, YY "Effect of cross-sectional aspect ratio on the strength of CFRP-confined rectangular concrete columns", Engineering Structures 32 (2010): 32-45.

[4] El-Hacha, R., and Abdelrahman, K. "Slenderness effect of circular concrete specimens confined with SFRP sheets", Composites Part B: Engineering 44 (2013): 152-166.

[5] Al-Salloum, Y. "Influence of Edge Sharpness on The Strength of Square Concrete Columns Confined with FRP Composite Laminates", Composites Part B: Engineering 38 (2007): 640-650.

[6] Chaallal, O., Shahawy M., and Hassan, M. "Performance of Axially Loaded Short Rectangular Columns Strengthened with Carbon Fiber-Reinforced Polymer Wrapping", Journal of Composites for Construction 7(2003): 200-208.

[7] Ilki, A., Peker, O., Karamuk, E., Demir, C., and Kumbasar, N. "Axial behavior of columns retrofitted with FRP composites", Advances in Earthquake Engineering for Urban Risk Reduction, Springer 66 (2006): 301-316.

[8] Rochette, P., and Labossiere, P. "Axial testing of rectangular column models confined with composites", Journal of Composites for Construction 4 (2000): 129-136.

[9] ANSYS, User Manual, revision 5.4, Houston, PA, 1995.